

25. VERTICAL SEISMIC PROFILE INTO UPPER OCEANIC CRUST IN HOLE 504B¹

Stephen A. Swift,² Hartley Hoskins,² and Ralph A. Stephen²

ABSTRACT

Seismograms from vertical seismic profiles (VSP) on Ocean Drilling Program Legs 111 and 148 were merged. First arrival traveltimes picked on the best quality traces are equivocal in the sediment but suggest an average velocity of about 1.8 km/s for the lower 110 m of section. In basement, VSP velocities follow the trend of the sonic log velocities but are generally equal to the highest sonic velocities measured in an interval. The general trend of VSP velocity follows that of refraction velocities, but the decrease in gradient marking the seismic Layer 2/3 boundary occurs ~500 m shallower at Hole 504B than in the surrounding 1–2 km region and appears to correlate with the top of the sheeted dikes. A downgoing arrival with velocities of 3–4 km/s is interpreted as a shear wave converted either by rough basement surface near the borehole or by shallow-buried lateral velocity variations. Several other arrivals can be most easily explained as coherent energy scattered from basement roughness or velocity inhomogeneities within the upper 500 m of basement. Downhole increases in VSP velocities correlate with events in the upgoing wavefield suggesting internal crustal reflections, but the amplitudes are no greater than side-scattered energy and coherency is generally poor over borehole depths exceeding 100–200 m.

INTRODUCTION

The relationship between seismic and geologic structure is very important to the investigation of upper crustal structure because seismic surveys remain the only cost-effective tool for investigating structure below the seafloor. The vertical seismic profile (VSP) is one of the key tools in determining this relationship. The VSP geometry differs from underway geophysical surveying. Whereas the sound source is a commonly used marine geophysical survey source, the receiver is a seismometer clamped in a borehole. The frequencies and length scales of the experiment are, thus, similar to those employed in seismic surveys, but the results can be related directly to the results of coring and logging in the borehole. Being the deepest penetration into upper ocean crust, the vertical seismic profile at Hole 504B offers the best opportunity to date to relate the geology of upper crust to seismic parameters.

Refraction investigations at Hole 504B by Hobart et al. (1985) and Collins et al. (1989) using sonobuoy receivers provide limited control on upper crustal structure because first arrivals from energy refracted in the upper half kilometer are obscured by higher amplitude reflections from the seafloor and the sediment-basement interface. These studies first showed relatively high amplitude shear arrivals at this site, and Collins et al. (1989) used shear amplitudes to constrain the compressional velocity at the top of basement. Both sonobuoy studies found the compressional velocity at the top of seismic Layer 3 is about 6.5 km/s. Collins et al. (1989) placed the Layer 2/3 boundary near 1.16 km depth below basement whereas Hobart et al. (1985) placed it somewhat deeper, near 1.4–1.5 km.

Alternatively, direct wave and diving wave arrivals propagating through the uppermost crust are clearly observed when the receiver is clamped within the borehole during oblique seismic experiments (OSE). OSEs were done at Hole 504B on Deep Sea Drilling Project (DSDP) Legs 70 and 92, and the velocities determined by traveltime inversions are well controlled, giving 4.3 km/s at the top of basement and a 1.2-km-thick layer with a vertical velocity gradient of 1.73 km/

s/km (Stephen and Harding, 1983; Little and Stephen, 1985). However, careful synthetic seismogram modeling of these same data indicated that significant velocity variations with scales of 1–3 km occur within 6 km of the hole (Stephen, 1988). Since the inversion results of Little and Stephen (1985) included arrivals passing through these structures, their velocity profile may not represent the seismic structure at the borehole. Detrick et al. (1994) recently re-examined seismic studies done at Hole 504B. They argued that the boundary between traditional seismic Layers 2 and 3 is determined by a downward decrease in velocity gradient and placed this boundary at 1500 ± 200 mbsf, within the sheeted dike sequence.

The first VSP in Hole 504B was shot during Leg 111 with clamping depths ranging from 161 mbsf in the cased sediment section down to 1526 mbsf in the sheeted dikes. Stacked seismograms presented in Shipboard Scientific Party (1988) show several upward-traveling events. Only one of the events interpreted as reflections from within basement were coherent over most receivers above the intercept with the borehole. The arrival with the largest amplitude and greatest vertical coherence was labeled "X" and was interpreted as a reflection from a dipping interface thought to intersect the projected borehole at a depth of 2038 mbsf (Shipboard Scientific Party, 1988, table 36).

On Ocean Drilling Program (ODP) Leg 148 a second VSP was shot from the maximum borehole depth (2076 mbsf) upwards to the base of the Leg 111 VSP (1516 mbsf). In this paper we combine the seismograms collected on both legs. We determine compressional wave velocities in sediment and basement from first arrival traveltimes. We also present preliminary velocities from weak shear arrivals in the upper 815 m of basement. We use frequency-wavenumber filtering to improve the image of coherent upgoing events, but many events interpreted as reflectors in Shipboard Scientific Party (1988) could not be resolved. We argue, instead, that much of the late arrivals are energy scattered by basement topography and lateral heterogeneities.

VSP EXPERIMENTS

Both VSP experiments on Legs 111 and 148 (see Shipboard Scientific Party, 1988, and Shipboard Scientific Party, 1993, for detailed descriptions) used the WST-A vertical component seismic tool, and both experiments recorded data sampled at 1 ms for 3 s with a nominal clamping interval of 10 m. During Leg 148, 6–10 shots were re-

¹Alt, J.C., Kinoshita, H., Stokking, L.B., and Michael, P.J. (Eds.), 1996. *Proc. ODP, Sci. Results*, 148: College Station, TX (Ocean Drilling Program).

²Department of Geology and Geophysics, Woods Hole Oceanographic Institution, Woods Hole, MA 02543, U.S.A. Swift: steve@heron.whoi.edu; Hoskins: hhoskins@whoi.edu; Stephen: rstphen@whoi.edu

corded at each depth, and during Leg 111, 1–75 shots (typically 8–25) were recorded. During Leg 111, a 950-in.³ air gun hung at 4.5 m below the sea surface and fired at 2000 psi was used as a sound source, whereas on Leg 148 the source was a 300-in.³ air gun hung at a depth of 6.7 m and fired at 1500 psi. Ancillary observations with a source monitor hydrophone suggest that the Leg 148 source signature is complicated by the interaction with the ship's hull (Hoskins, this volume). Figure 1 compares the direct wave trace and power spectrum for traces taken from adjacent borehole depths. The difference in source depth and volume and the interaction with the ship's hull produces markedly different seismograms at essentially the same depth. Relative to the high energy peak at about 55 Hz, there are differences of up to 20 dB in the band below 60–70 Hz. The most significant spectral difference occurs above 70 Hz where coherence between receiver depths is poor. The lower energy in the Leg 148 spectra above 70 Hz indicates quieter experimental conditions; the source of the Leg 111 noise is unknown.

Preliminary processing of the data used in this study was handled somewhat differently for each leg. The original Leg 111 data were unavailable in seismic data exchange format. In 1992, copies of the Leg 111 field tapes stored at ODP were reformatted to SEG Y exchange tapes at Schlumberger Well Services, New Orleans. The Leg 148 field tapes were reformatted to SEG Y files using software at ODP by M. Weiderspahn, UT-A. Presumably, any changes in gains applied to the recorded seismograms during the experiment were removed by software during acquisition and this preprocessing step. We will show below, however, that the Leg 111 data still contain uncorrected gain changes.

RECORD SECTIONS

Sediment

The complete sediment section was not covered during Leg 111 and time was too short on Leg 148 to reshoot the section. The traces at ~186 mbsf have obvious timing errors (Fig. 2A). Velocities determined from first arrivals in the traces at 246 m, 250 m, and 254 mbsf are unreasonably high or low for the sediment lithologies recovered, so these traces may also have errors in the recorded delay time. These traces were recorded in steel casing where tool slippage problems were reported by Shipboard Scientific Party (1988), but it is unlikely the depth errors of up to 20 m required to get reasonable velocities went unrecorded. The reflection off the top of basement is a doublet that we interpret as the summation of two separate reflections separated by about 11 ms. A second downgoing event appears at 0.17–0.175 s behind the direct wave (Fig. 2). This phase does not have the double pulse waveform and is most likely the first bubble pulse. The doublet is likely a result of a reflection off the top of the basal limestone/chert layer at the site. No sonic logs are available at Holes 501 and 504A, but density logs indicate a 35-m-thick layer of limestone with a density change of about 0.3 g/cm³ at the top (Cann and Von Herzen, 1983, figs. 2, 3). If the layer is also 35 m thick at Hole 504B the top should be at a depth of about 240 mbsf (basement at Hole 504B was recorded as 274.5 mbsf near the bottom of Core 69-504B-2R by the Shipboard Scientific Parties, 1983). The decrease in peak amplitude of the direct wave, however, does not occur until the trace at 250 m (Fig. 2C), so the layer at Hole 504B has a maximum thickness of 28 m. Thus, the limestone layer is no thicker at Hole 504B where basement is deepest relative to sea level indicating uniform sedimentation patterns within the basement basin where Hole 504B is located.

Basement

The basement seismograms shot using an air gun source were processed to improve signal/noise. All traces from both legs were plotted

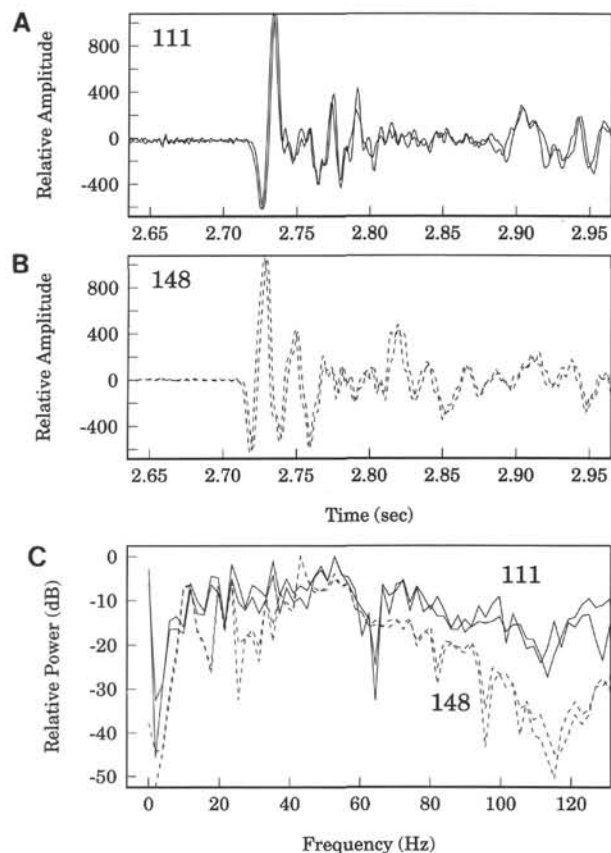


Figure 1. Comparison of seismograms from (A) Leg 111 (stacked traces from 1506 and 1519 mbsf) and (B) Leg 148 (stacked traces from 1516 and 1526 mbsf) shows distinct differences in waveforms. (The Leg 111 amplitudes are scaled by 10^{-5} to equalize the peak amplitudes.) Because the traces are so close together in a portion of the borehole where lithology varies little with depth, most differences in the traces can be ascribed to the difference in source used. The timing shift discovered in the traveltime picks has not been applied. C. Power spectrum of the initial 0.512 s of data in each of the two traces. The Leg 111 spectra (solid) shows higher noise levels at frequencies greater than 70 Hz than the Leg 148 spectra (dashed). More importantly, differences of 10–20 dB occur at 12–20 Hz and at 25–35 Hz.

and 3–5 traces at each depth with the best signal/noise were selected by inspection and stacked. At several depths in the Leg 111 data all available traces were poor quality as a result of contamination by large amplitude, sporadic banging possibly caused by debris falling from shallower in the hole; these depths were eliminated from the final stacked section. Occasionally air gun shots were collected at spacing closer than 10 m. For these cases, we retained only the traces at the receiver depth that had the highest signal/noise and that best maintained the 10-m nominal borehole depth spacing. A constant scaling factor was applied to match amplitudes at the boundary between the two data sets and a static time delay of 7.5 ms was added to the Leg 148 seismograms to match first arrival times (see below).

Several features of the data are immediately apparent in the joint, unfiltered record section (Fig. 3). Seismograms at the deepest four receiver depths in the Leg 111 data were too noisy to use, so there is overlap of only one receiver depth at ~1520 mbsf. Ringing at about 110 Hz is more common above ~900 m, where the hole diameter is enlarged and irregular owing to caving of poorly consolidated pillows. We agree with the Shipboard Scientific Party (1988, p. 128) that the ringing is probably the result of tool resonance caused by

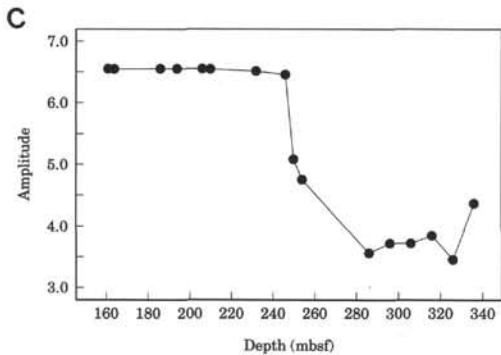
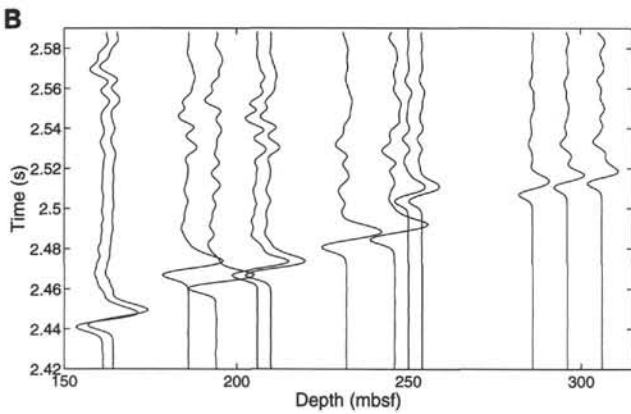
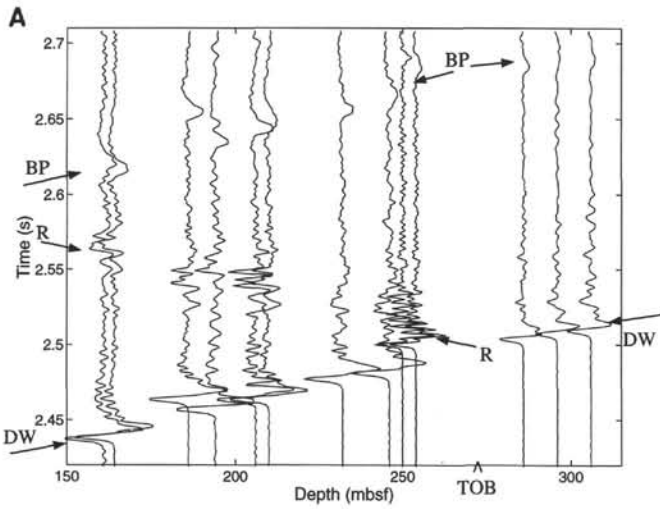


Figure 2. Seismograms collected on Leg 111 in the cased sediment section. The top of basement (TOB) is at 274.5 mbsf, and the three right traces are in basement. Note probable timing errors of traces at 186, 250, and 254 mbsf. The arrival times of the direct wave (DW) and the bubble pulse (BP) increase with depth, whereas the arrival time of the basement reflection (R) decreases with increasing depth. **A.** Unfiltered stacked seismograms. **B.** Stacked seismograms after low pass filtering using a minimum phase Butterworth filter with a corner frequency of 90 Hz and 3 poles. The time scale is expanded to show the doublet in the reflected phase. **C.** Peak-to-peak amplitude of the direct wave arrival in the sediment section and the upper basement showing the loss of amplitude at 250 mbsf (interpreted as a reflection from the top of the limestone/chert layer) and the top of basement.

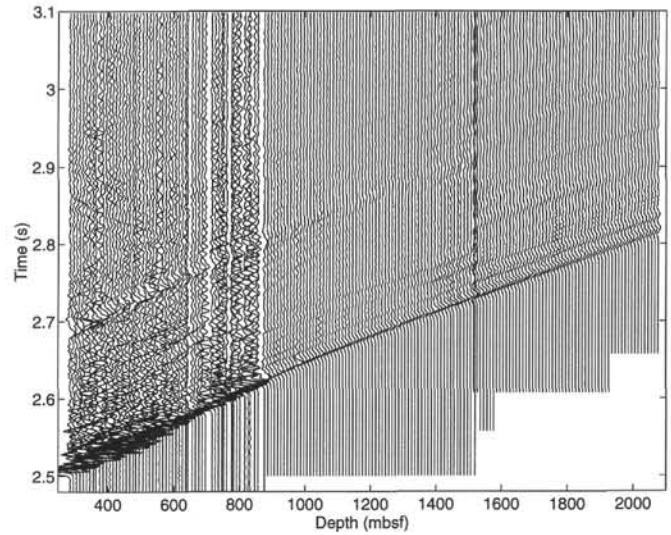


Figure 3. Unfiltered seismograms from both legs merged together. Corrections include scaling the amplitudes of the Leg 148 seismograms by 10^5 to match the amplitude of traces near 1516–1519 m and time shifting the Leg 148 seismograms by +7.5 ms.

poor clamping. Amplitudes decrease downward at ~880 mbsf and increase at ~1390 mbsf. Figure 4 shows that there is nearly identical decrease in the amplitude of coda and the direct wave at 880 mbsf. Root-mean square values also decrease by a similar amount and similar but more irregular results are obtained for the shorter noise section before the first arrival. These same quantities increase at ~1390 mbsf. The similarity of noise and signal amplitude changes leads us to conclude that a gain change was inadvertently preserved in the Leg 111 seismograms. We multiplied amplitudes at depths from 886 to 1386 mbsf by two. Figure 5 shows that this scaling eliminates a serious down-hole anomaly in both peak-to-peak amplitude and spectral power.

TRAVELTIME ANALYSIS

The first arriving direct wave moves across the VSP array at the compressional wave velocity of the formation. Traveltimes of the direct wave were picked in the low-noise seismograms used in the stacks. The high signal/noise in the data enabled picking to a precision of a few milliseconds (Fig. 6). At 1535 mbsf there is a traveltime offset between the data sets from the two legs, probably resulting from slight differences in acquisition parameters. A time shift of 7.5 ms applied to all Leg 148 seismograms produces a smooth traveltime curve.

The depth-to-depth variability in traveltime for the sediment portion of the VSP is up to four times the variability in basement traveltimes (Fig. 7). Physically unrealistic velocities are implied by the traveltime “inversions” between 186 and 194 mbsf and between 206 and 210 mbsf and by the traveltime delay between 246 and 250 mbsf. The traveltimes at 254 and 286 mbsf across the top of basement require a velocity of 9.2 km/s. We conclude that much of the traveltime variability is caused by errors in timing. We do not know the source of the timing errors. A small portion of the anomalies may result from incorrect logging of the seismometer depth in the shot headers after slippage of the tool in the casing set between the seafloor and the top of basement on DSDP Leg 69. Shipboard Scientific Party (1988) noted that the tool slipped “a few meters” before a secure clamping could be obtained and attributed the problem to a broken tooth on the clamping arm. However, errors of 15–20 m are required to explain the traveltimes at 186, 250, and 254 mbsf. Clearly, some other source of error was introduced by the change from clamping in basement to

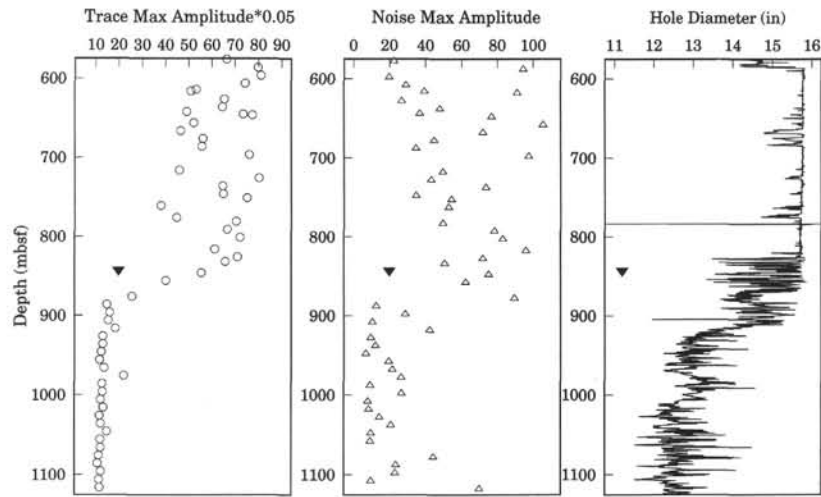


Figure 4. Comparison of signal and noise amplitudes across the large amplitude change in the Leg 111 data. The left panel shows the maximum amplitude (scaled by 0.05) for the whole trace. For most traces this value is the amplitude of the direct wave. Note the change from ~15 to ~60 at about 875 mbsf. The second panel shows maximum amplitude in one second of coda beginning 1.5 s after the direct wave arrival. Note the change from ~15 to ~60 at 875 mbsf. The change occurs at the same depth and is the same factor indicating that there is an instrument gain change affecting the whole trace and not just an early arrival. Similar results were obtained when root-mean square values were computed and when the ~0.5 s before the arrival of the direct wave was studied. Above the triangle are pillows; below are mixed pillows and sheeted dikes ("transition zone"; Becker et al., 1989). The right panel shows the unfiltered caliper log from the Formation MicroScanner run during Leg 148.

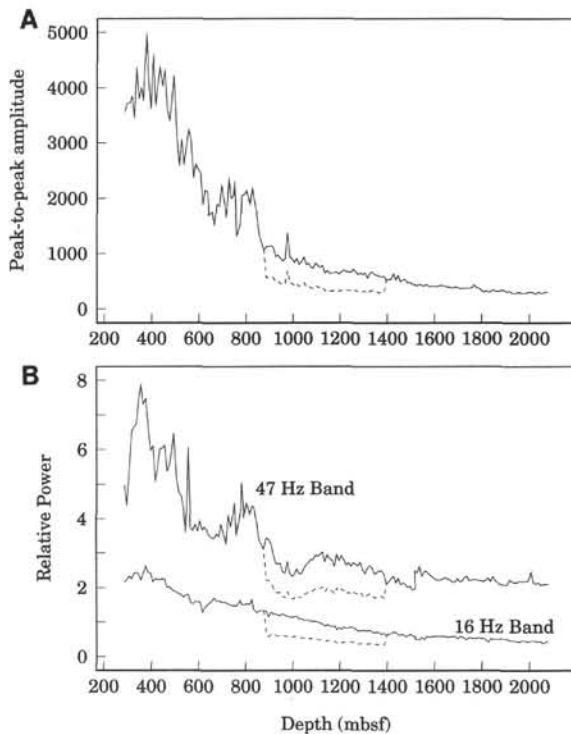


Figure 5. The effect of scaling the amplitudes of the Leg 111 traces between 886 and 1386 by a factor of two is to smooth the downhole variation of (A) peak-to-peak amplitude in the direct wave and (B) spectral power in 15.6 Hz bands near the peak energy of the source. Dashed line shows values before correction; solid line is after the correction. Spectra were computed on 0.1 s of signal after the first arrival using tapering and padding to 128 points.

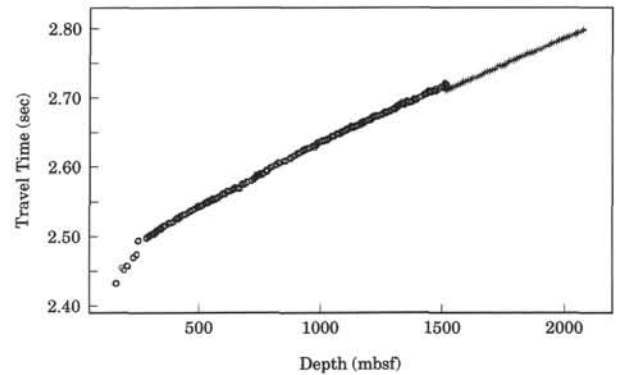


Figure 6. Traveltime picks for the highest quality seismograms at each depth for which good seismograms were available. The Leg 148 direct wave (plus signs) arrived about 7.5 ms earlier than the Leg 111 direct wave (circles).

clamping in casing, but its nature and size can not be determined from the data available to us. Careful inspection of the traveltime variability in the data indicates that a change in velocity at the top of the limestone/chert layer, identified above on the basis of amplitudes, cannot be reliably determined.

Shipboard Scientific Party (1988, table 35, p. 149) used the traveltime difference between the seafloor echo and the uppermost VSP receivers to obtain a realistic velocity of 1.586 km/s for the upper half of the sediment column. Figure 7 shows that this velocity is not consistent with the VSP traveltimes and should not be extrapolated to deeper depths. We obtain a velocity of 1.81 km/s for the lower half of the column using the traveltimes to the uppermost VSP receiver and to basement (estimated by projecting basement velocity upwards to 274.5 mbsf; Fig. 7). The greatest source of error arises from averaging velocities across the lithology change between the chalk and the limestone/chert units. The error in our velocity is less than 1% resulting from the misidentification of the depth to basement in DSDP Core 69-504B-2R and from possible slowing of basement velocity above the

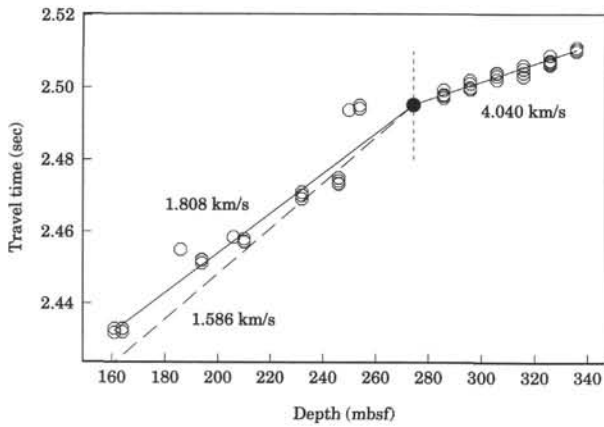


Figure 7. Open circles are first-arrival picks for the Leg 111 seismograms with the best signal/noise. The basement velocity of 4.04 km/s (solid line), computed using the mean traveltimes from the stations at 286 and 336 mbsf, is extrapolated up to 274.5 mbsf (vertical short dash line) to obtain the traveltime at the base of the sediments (solid circle). This traveltime and the mean traveltime at 161 mbsf give the velocity of 1.81 km/s shown by the solid line. The velocity of 1.586 km/s (long dashed line) determined for the sediment layer above 161 m by Shipboard Scientific Party (1988) cannot explain the VSP traveltimes below 161 mbsf.

shallowest basement receiver at 286 mbsf. The location of the boundary between the 1.58 and 1.81 km/s layers may be the downward transition from ooze to nanofossil chalk at 143 mbsf (Shipboard Scientific Parties, 1983).

Traveltimes in basement, reduced with a velocity of 5.5 km/s, show several relatively linear segments (Fig. 8). Because of the picking error the depth limits of the segments are constrained to about ± 25 m. We fit straight lines to the original traveltimes in each segment to estimate interval velocities (Table 1). Finer depth subdivision of the segments is unwarranted given the scatter in traveltimes.

WAVEFIELD IMAGING

Several interesting features can be seen in the processed basement record section combining Legs 111 and 148 (Fig. 9). The bubble pulse parallels the direct wave arrival with a 0.18 s delay. Several weak upgoing events can be identified above 1200 mbsf; none, however, are coherent across the array to intersect the direct wave. The latest arriving event, intercepting the sediment-basement contact at about 3.05 s, is the curved event "X" identified by the Leg 111 Shipboard Scientific Party (1988). A weak downgoing arrival (Sh), intercepting the direct wave at the top of basement and dipping at a low velocity away from the direct wave, can be traced to a depth of about 1100 mbsf. Lastly, an arrival (Sc) appears about 0.08 s behind the direct wave at about 880 mbsf and gets closer to the direct wave with increasing depth.

To better image the arrivals, upgoing and downgoing wavefields were separated using frequency-wavenumber (f_k) filtering (Christie et al., 1983; Hardage, 1983, p. 174–182; Swift et al., 1991; Bolmer et al., 1992). The stacked traces from the two legs were filtered separately because of the significant differences in the source waveforms. For each leg the traces were scaled to equalize the maximum amplitudes and lowpass filtered at 70 Hz. The data were padded and tapered with sine-squared functions and the quadrant mutes were tapered to minimize edge effects and aliasing.

In the downgoing wavefield, the low-velocity arrival intercepting the top of basement at the same time as the direct wave is more clear (Fig. 10). We varied plotting parameters, bandpass filters, and gain

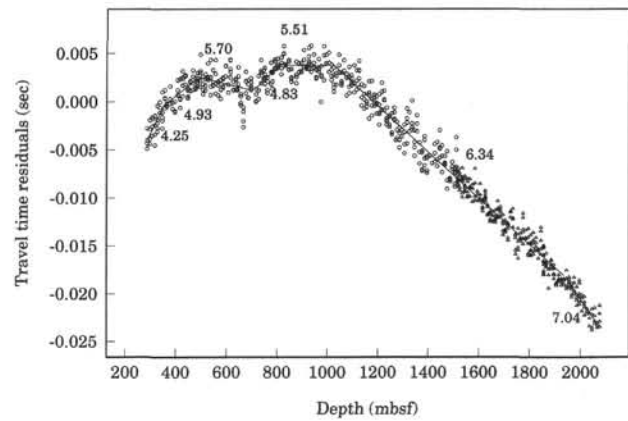


Figure 8. Traveltime residuals for the Leg 111 (circles) and Leg 148 (triangles) basement section. The Leg 148 data were corrected by adding 7.5 ms. Traveltimes in Figure 6 were adjusted by subtracting a straight line which removed a trend corresponding to a velocity of 5.5 km/s. The residuals were subdivided by eye. The original traveltimes were fit using linear regression (solid lines) giving the labeled velocities in km/s and uncertainties listed in Table 1.

Table 1. Velocities at Hole 504B from VSP traveltime analysis.

Depth to base of layer (mbsf)	Compressional-wave velocity (km/s)	95% Confidence limits (km/s)
274	1.81	
360	4.25	3.98–4.56
480	4.93	4.74–5.13
700	5.70	5.59–5.82
825	4.83	4.63–5.05
1000	5.52	5.36–5.67
1946	6.34	6.32–6.35
2076	7.04	6.83–7.26
Depth to base of layer (mbsf)	Shear velocity (km/s)	
975	2.95	
1095	3.85	

Note: The regression slopes and uncertainties were computed in the slowness domain and converted to velocity for this table.

control, but the arrival could not be imaged clear enough to pick individual traces. The graphically measured velocity is ~ 3 km/s down to 975 mbsf and ~ 4 km/s below (Table 1). These velocities are similar to shear-wave velocities measured in upper ocean crust (Spudich and Orcutt, 1980). Observation of shear energy with a vertical component geophone at near-normal incidence is unexpected because the compressional wave in water and sediment should produce vertically directed compressional particle motion on a flat, uniform basement surface. Its appearance in our VSP is likely caused by an irregular basement surface at the borehole site.

In the upgoing wavefield (Fig. 11) weak events are more apparent than in the unprocessed section, but only events intersecting the borehole at depths less than ~ 1000 mbsf are coherent across the array of overlying receivers. Most of these events intercept the borehole near depths where changes in velocity were interpreted from the traveltime data (Fig. 8; Table 1) and, thus, are probably reflections. The lack of coherency elsewhere is caused by poor signal/noise and, to a lesser extent, to aliased energy from the direct wave and the bubble pulse. The two events with the most coherency across the array intercept the borehole at about 600 m and 950 mbsf. The former event

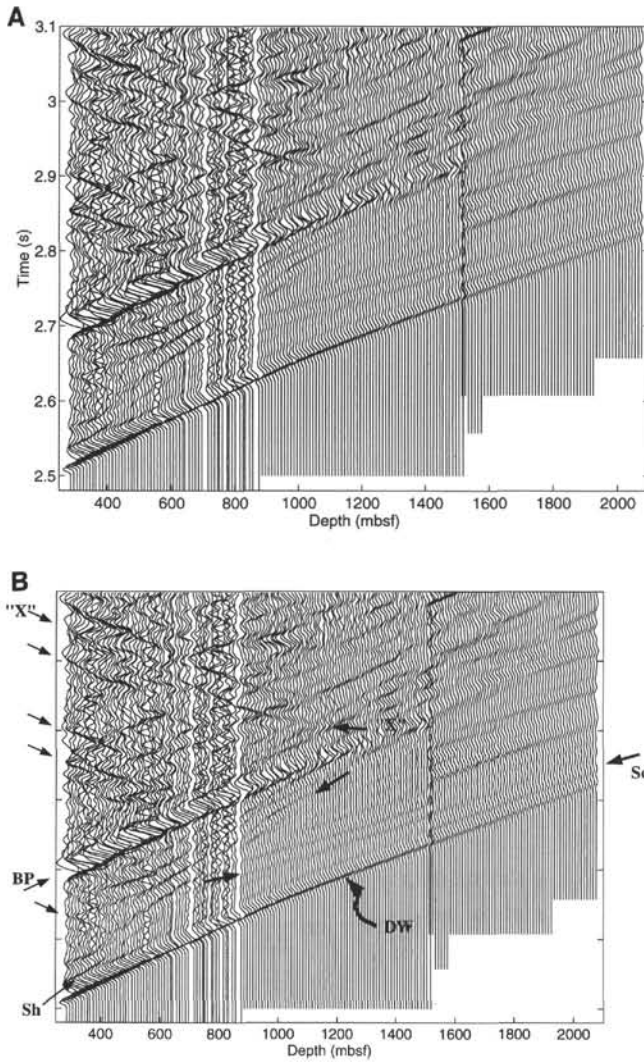


Figure 9. **A.** The combined VSP record section showing stacked traces after a factor of two gain change was applied to traces from 886 m to 1386 mbsf. The seismograms were processed with a lowpass, minimum phase Butterworth filter using a corner frequency of 50 Hz and three poles and a time-varying gain filter with a window of 0.05 s. **B.** Arrows have been added to the image in Figure 9A to indicate downgoing events: DW = direct wave, Sh = shear-wave event, BP = bubble pulse, and Sc = an event that moves across the array with a velocity higher than the direct wave but arrives after the direct wave. Upgoing events have an opposite slope and are marked with arrows on the time axis. The curved event "X" identified as a reflection off a dipping fault by Shipboard Scientific Party (1988) is marked by arrows.

(dashed arrow in Fig. 11) may be a reflection from a 10- to 20-m thick layer at 655–665 mbsf characterized in Figure 8 by unusually early traveltimes arrivals. The event at 950 mbsf is the highest amplitude event imaged and appears across 450 m of borehole depth. This event is probably a reflection and supports the interpretation above that a sharp step in velocity occurs coincident with the top of the sheeted dike unit in Hole 504B. Below 1000 mbsf, the amplitude of events at 1550, 1680, and 2050 mbsf (asterisks in Fig. 11) is lost in noise in overlying receivers after less than 100 m. Lack of coherence of the deeper events could result from destructive interference with energy scattered laterally from velocity inhomogeneities located above the reflecting surface and from the side of the borehole. Attenuation seems an unlikely explanation in view of the minimal change in the

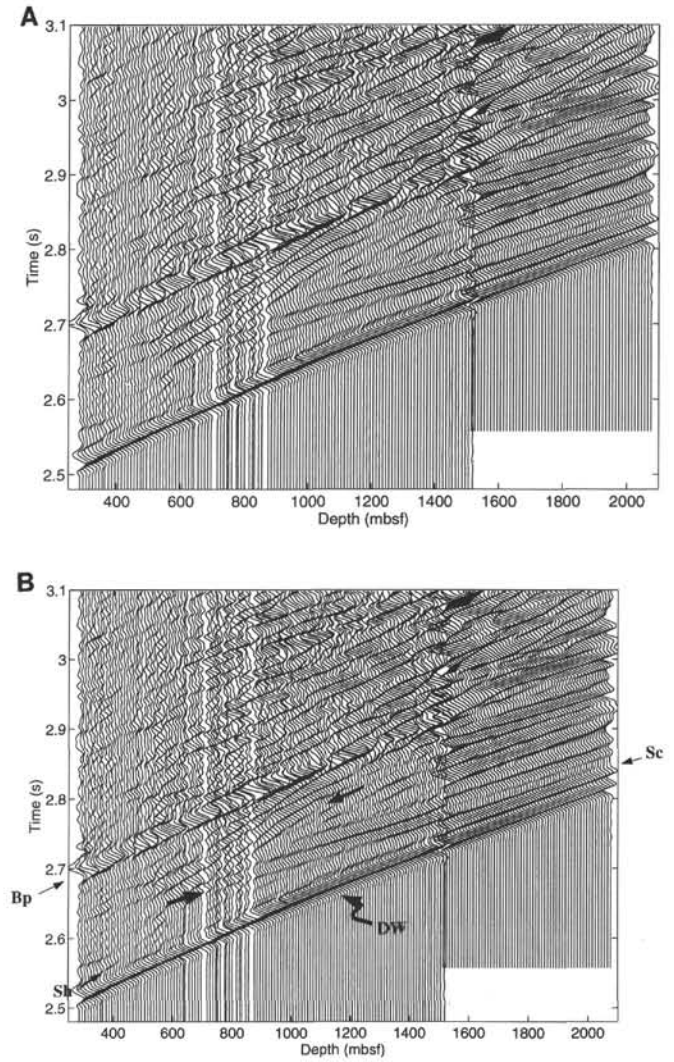


Figure 10. The downgoing wavefield. After amplitudes in the stacked traces were adjusted to equalize maximum amplitudes and bandpass filtered with corner frequencies of 5 and 70 Hz, the section was fk filtered to null the upgoing energy. **A.** Filtered traces. **B.** Filtered traces labeled with arrows to indicate the direct wave (DW), shear-wave event (Sh), bubble pulse (BP), and an event (Sc) that moves across the array with a velocity higher than the direct wave but arrives after the direct wave.

amplitude of the direct wave with range at these depths. We suggest below that coherent events that *do not* intersect the borehole, including event "X" which is coherent only between 1150 and 600 mbsf, may be energy scattered from rough basement topography or from sub-basement inhomogeneities.

DISCUSSION

Typically velocities derived from VSP traveltimes are more closely related to the geology recovered from the borehole than velocities from refraction experiments which use sources offset from the borehole and represent larger-scale, horizontal averages of velocity. The basement VSP velocities at Hole 504B do, indeed, more closely approximate velocities measured within a meter of the borehole by the sonic log than do refraction results (Fig. 12). Although, sonic and VSP velocity measurements have different depth resolu-

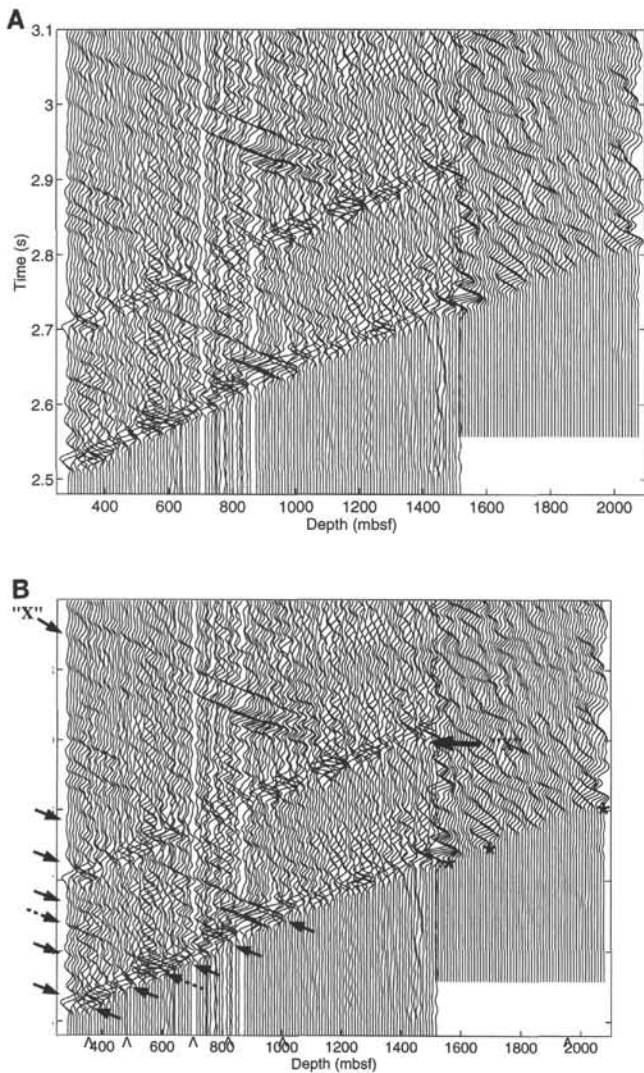


Figure 11. The upgoing wavefield. Amplitudes in the stacked traces were adjusted to equalize maximum amplitudes, bandpass filtered (minimum phase) with corner frequencies of 5 and 70 Hz, and then the section was f_k filtered to null the downgoing energy. The display was lowpass filtered with a corner frequency of 50 Hz. The gain here is ten times that in Figure 10. **A.** Filtered traces. **B.** Filtered traces labeled with solid arrows to indicate upgoing events that correlate with steps in VSP velocities, marked on the depth scale by inverted "V"s. The curved event "X" identified as a reflection off a dipping fault by Shipboard Scientific Party (1988) is marked with solid arrows. Asterisks mark locations along the trace of the direct wave where high-amplitude, upgoing energy is coherent for about 100 m.

tion, the results of the two methods generally agree. The VSP velocities are generally equal to the highest peak velocities reached by the sonic log in any interval. The exceptions are two depth intervals where the Leg 148 sonic log decreases: 274–360 and 700–825 mbsf. In these intervals, the straight line fits used to obtain the VSP velocities may have been inadequate to resolve the curvature in travel-times. In the deeper interval a velocity gradient may be a better model than a constant velocity layer. A velocity gradient would give smaller reflection coefficients, which is consistent with low amplitude of the upgoing energy from 700 and 850 mbsf borehole depths (Fig. 11). In the 274–360 mbsf layer, the VSP traveltimes clearly indicate velocities between 4.0 and 4.5 km/s (Figs. 7, 8). Figure 13 shows that this

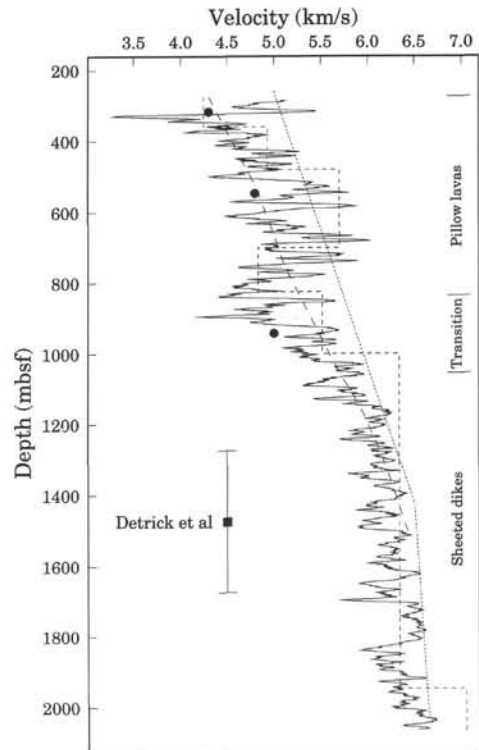


Figure 12. Comparison of VSP velocities from Table 1 (short dashed line) with the sonic log (solid line, smoothed with a 7.5-m running average). Refraction velocities from Collins et al. (1989) are shown with a dotted line and OSE velocities from Little and Stephen (1985) by a long dashed line. Solid circles are inflection point velocity determinations from Little and Stephen (1985). The large bracket indicates the seismic Layer 2/3 transition estimated by Detrick et al. (1994). Generalized borehole lithology along the right margin is from Becker et al. (1989).

is the only depth interval in which sonic log velocities *increase* between Legs 111 and 148 (Fig. 13). This is the opposite effect that is expected from the breakdown of the borehole walls. The VSP velocities match the Leg 111 sonic log better than the Leg 148 sonic log, but the quality of the logs in this interval is too unreliable to justify a more detailed comparison.

In most layers the 95% confidence interval of the VSP velocities lie near the maximum values of the sonic log for the same interval (Fig. 12; Table 1). Stewart et al. (1984) discuss sources of error for sonic log and VSP velocities and the reasons for discrepancies. The most likely explanation for the Hole 504B data is that "lateral formation changes with higher velocities will allow the seismic energy to follow a faster path" (Stewart et al., 1984, p. 1168, item h). Presumably, seismic energy travels vertically at velocities equivalent to the maximum velocities for that layer within a seismic wavelength. A more detailed examination of this hypothesis is beyond the scope of this paper. Stewart et al. (1984) also suggest that decay of borehole conditions and packing of the borehole wall by drilling mud may reduce borehole wall velocity measured by the sonic log; this, presumably could have occurred by reentry and drilling on Legs 137, 140, and 148. Figure 13 shows, however, that although the borehole wall has changed shape (note especially the changes between 600 m and 700 mbsf), there has been little change in the sonic log velocity when averaged over 7.5 m.

The VSP velocities do not differ greatly from the magnitude and trend of velocities determined by the OSE at Hole 504B (Fig. 12). Both have a velocity of ~4.3 km/s near the top of basement, and both

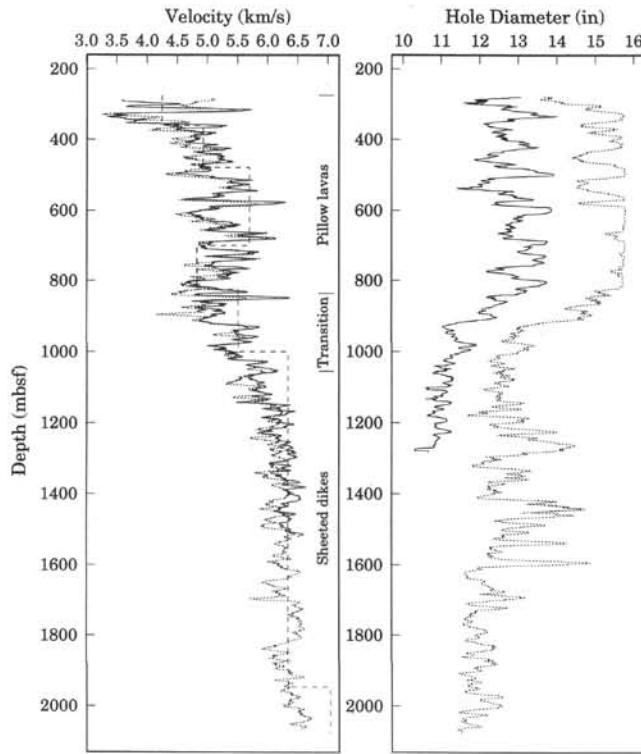


Figure 13. Comparison of sonic logs and "caliper" logs for Legs 111 (solid lines) and 148 (dotted) from the Borehole Research Group/LDEO. VSP velocities (dashed) and lithology as in Figure 12. Hole diameter for the two legs have not been intercalibrated: the Leg 111 was computed from borehole televiewer data, whereas the Leg 148 data comes from the Formation Micro-Scanner tool. Although the absolute diameters cannot be compared the relative changes in diameter downhole probably reflect real changes in the condition of the borehole caused by drilling activities on Legs 137, 140, and 148.

have velocities of ~6.4 near 1500 mbsf. VSP velocity increases somewhat more rapidly with depth and the vertical gradient changes near 1000 mbsf rather than at ~1500 mbsf. The sharpness of the step in VSP velocity at 1000 mbsf is problematic. The traveltimes in Figure 8 allow the transition from the 5.5 km/s layer above to the 6.3 km/s layer below to be gradational above 1100 m smoothing the step and lowering the VSP velocities to levels closer to sonic log velocities. The relatively high amplitude of the energy reflected from this depth in Figure 11, however, suggests that a sharp change in physical properties occurs at this depth consistent with the interpretation in Figures 8 and 12.

If a change in the vertical gradient of velocity is used to define the seismic Layer 2/3 boundary, as argued by Detrick et al. (1994), then the boundary at the hole detected by the VSP seems somewhat more shallow than the region within 1–2 km of the borehole sampled by the OSE ray paths. If this is true, then Layer 2/3 boundary topography of 200–500 m exists over a broad range of lateral wave numbers. Figure 14 shows a schematic view of how vertical variations in the boundary could produce the velocity profiles shown in Figure 12. Another consequence of defining the Layer 2/3 boundary as a change in the VSP velocity gradient is that the boundary occurs within the lithologic transition zone only about 50 m above the top of the sheeted dike section. It is important to note that the VSP velocity of 6.3 km/s in the 1000–1946 mbsf interval is consistent with the 6.5 km/s velocity for upper seismic Layer 3 determined by Collins et al. (1989), given the traveltime variability cited in their Figure 4.

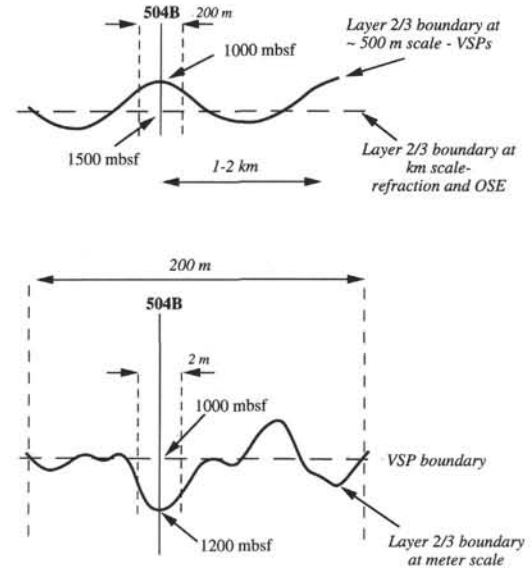


Figure 14. Schematic diagram to show an interpretation of the seismic Layer 2/3 boundary on the basis of observations made using different methods. The depth to the seismic Layer 2/3 boundary depends on the scale of observation. In the upper panel, the Layer 2/3 boundary defined by refraction methods appears flat on lateral scales of 1–2 km whereas the boundary seen by the VSP method over finer scales has topography of hundreds of meters. At smaller length scales in the lower panel, the VSP boundary appears flat, whereas the local boundary position determined from the sonic log also has topography of a few hundred meters. At the refraction and OSE scale the velocity-depth function is best represented by gradients. At the VSP scale the velocity-depth function is best represented by thick homogeneous layers.

If events in the upgoing wavefield are reflections from surfaces intersecting the borehole, the VSP velocity should change at the depths of intersection. Figure 11 shows weak but coherent reflections near the bases of the shallowest VSP velocity layers at 360 and 490 mbsf. The event at 700 mbsf is very weak and only coherent across receiver depths between 300 and 400 mbsf. At 825 mbsf a reflection can be traced upwards 100–150 m but is weak and lacks coherence above 650–700 mbsf. Near 1000 mbsf an event coherent up to ~600 mbsf can be traced. There is no convincingly coherent amplitude event at the velocity change near 1940 mbsf. With the exception of the 1940 mbsf velocity change, the correlations occur when VSP velocity increases with depth but not when VSP velocity decreases.

The correlation of coherent events in Figure 11 with borehole depths where VSP velocity changes indicates that some of the events in the image of upgoing wavefield are energy reflected from velocity discontinuities. Other coherent events, including event "X," cannot be traced downhole to intersect the direct wave (Fig. 11). If a reflecting surface intersects the borehole, then the amplitude of its reflection should be greatest in receivers immediately above the depth of intersection. Thus, it is unlikely that these events are reflections, and some are probably the result of scattering from inhomogeneities within the adjacent formation or from roughness of the sediment-basement contact. Dougherty and Stephen (1991) proposed that curvature of events in VSP images could be explained by scattering. With a simple representation of a rough seafloor they were able to produce a synthetic VSP image with events (Dougherty and Stephen, 1991, fig. 8) that are similar in amplitude relative to the downgoing energy, curvature, and depth coherence to the events in Figure 11.

Several other lines of evidence in the VSP images argue for scattered energy. The occurrence of a downgoing event with velocity

similar to upper crustal shear-wave velocity and an intercept time near the top of basement indicates that shallow-buried lateral velocity heterogeneities exist or that basement topography near the borehole is sufficiently rough to scatter compressional wave energy. The discontinuities in upgoing events and their failure in many examples to intercept the borehole suggests the energy is not a reflection from an impedance contrast intersecting the borehole or that scattered energy is significant enough to interfere destructively with propagation over depth intervals of several hundred meters. Lastly, the high velocity, downgoing arrival can only be explained as energy propagating downward from a source located away from the borehole above 500 mbsf (Fig. 10). Amplitudes of scattered energy (e.g., event "X" in Fig. 11) seem to equal or exceed amplitudes of events which can be interpreted as true reflections by their coherence and by correlating them to downhole increase in VSP velocity (e.g., the reflection at 1000 mbsf).

CONCLUSIONS

In general, VSP velocities follow the trend of the sonic log over length scales of 100–300 m but are equal to the highest sonic velocities measured in an interval. VSP velocities increase downward with a gradient equal to that of refraction velocities but the change in gradient is shallower by about 500 m and is located at ~1000 mbsf near the top of the sheeted dike section. Weak reflection events appear to correlate with most downward increases in velocity gradient, but the array coherence of deeper events is only 100–200 m. Converted shear waves are observed in the downgoing wavefield. Energy scattered by irregularities on the top of basement or shallow-buried velocity inhomogeneities equals or exceeds the amplitude to events most easily interpreted as reflections.

ACKNOWLEDGMENTS

We thank the crew and ODP personnel aboard ODP Leg 148 for their assistance and cooperation in collecting the VSP. Steven Kirtledge, Schlumberger engineer, made the measurements. Mark Weiderspahn, UT-A, kindly provided and operated the code to reformat Leg 148 VSP data from Schlumberger to SEG-Y. Graham Kent and Tom Bolmer provided additional computer support. We are grateful for the encouragement, criticism, and processing assistance given us by John Collins and Dan Lizarralde. Cristina Broglia, LDEO, kindly provided logs from Legs 111 and 148. Support was provided by NSF contract OCE 9313794 and purchase orders OCE 84-09478 (JOI Subaward 2-93 and USSSP 148-20778b). This is WHOI contribution number 8911.

REFERENCES

- Becker, K., Sakai, H., Adamson, A.C., Alexandrovich, J., Alt, J.C., Anderson, R.N., Bideau, D., Gable, R., Herzig, P.M., Houghton, S.D., Ishizuka, H., Kawahata, H., Kinoshita, H., Langseth, M.G., Lovell, M.A., Malpas, J., Masuda, H., Merrill, R.B., Morin, R.H., Mottl, M.J., Pariso, J.E., Pezard, P.A., Phillips, J.D., Sparks, J.W., and Uhlig, S., 1989. Drilling deep into young oceanic crust, Hole 504B, Costa Rica Rift. *Rev. Geophys.*, 27:79–102.
- Bolmer, S.T., Buffler, R.T., Hoskins, H., Stephen, R.A., and Swift, S.A., 1992. Vertical seismic profile at Site 765 and seismic reflectors in the Argo Abyssal Plain. In Gradstein, F.M., Ludden, J.N., et al., *Proc. ODP, Sci. Results*, 123: College Station, TX (Ocean Drilling Program), 583–600.
- Cann, J.R., and Von Herzen, R.P., 1983. Downhole logging at Deep Sea Drilling Program Sites 501, 504, and 505, near the Costa Rica Rift. In Cann, J.R., Langseth, M.G., Honnorez, J., Von Herzen, R.P., White, S.M., et al., *Init. Repts. DSDP*, 69: Washington (U.S. Govt. Printing Office), 281–300.
- Christie, P.A.F., Hughes, V.J., and Kennett, B.L.N., 1983. Velocity filtering of seismic reflection data. *First Break*, 1:9–24.
- Collins, J.A., Purdy, M.G., and Brocher, T.M., 1989. Seismic velocity structure at Deep Sea Drilling Project Site 504B, Panama Basin: evidence for thin oceanic crust. *J. Geophys. Res.*, 94:9283–9302.
- Detrick, R.S., Collins, J., Stephen, R., and Swift, S., 1994. *In situ* evidence for the nature of seismic Layer 2/3 boundary in oceanic crust. *Nature*, 370:288–290.
- Dougherty, M.E., and Stephen, R.A., 1991. Seismo/acoustic propagation through rough seafloors. *J. Acous. Soc. Am.*, 90:2637–2651.
- Hardage, B.A., 1983. *Vertical Seismic Profiling, Part A: Principles*: London (Geophysical Press).
- Hobart, M.A., Langseth, M.G., and Anderson, R.N., 1985. A geothermal and geophysical survey on the south flank of the Costa Rica Rift: Sites 504 and 505. In Anderson, R.N., Honnorez, J., Becker, K., et al., *Init. Repts. DSDP*, 83: Washington (U.S. Govt. Printing Office), 379–404.
- Little, S.A., and Stephen, R.A., 1985. Costa Rica Rift borehole seismic experiment, Deep Sea Drilling Project Hole 504B, Leg 92. In Anderson, R.N., Honnorez, J., et al., *Init. Repts. DSDP*, 83: Washington (U.S. Govt. Printing Office), 517–528.
- Shipboard Scientific Parties of Leg 68 (Site 501), Leg 69, and Leg 70, 1983. Sites 501 and 504: sediments and oceanic crust in an area of high heat flow on the southern flank of the Costa Rica Rift. In Cann, J.R., Langseth, M.G., Honnorez, J., Von Herzen, R.P., White, S.M., et al., *Init. Repts. DSDP*, 69: Washington (U.S. Govt. Printing Office), 31–173.
- Shipboard Scientific Party, 1988. Site 504: Costa Rica Rift. In Becker, K., Sakai, H., et al., *Proc. ODP, Init. Repts.*, 111: College Station, TX (Ocean Drilling Program), 35–251.
- , 1993. Site 504. In Alt, J.C., Kinoshita, H., Stokking, L.B., et al., *Proc. ODP, Init. Repts.*, 148: College Station, TX (Ocean Drilling Program), 27–121.
- Spudich, P., and Orcutt, J., 1980. A new look at the seismic velocity structure of the oceanic crust. *Rev. Geophys. Space Phys.*, 18:627–645.
- Stephen, R.A., 1988. Lateral heterogeneity in the upper oceanic crust at Deep Ocean Drilling Project Site 504. *J. Geophys. Res.*, 93:6571–6584.
- Stephen, R.A., and Harding, A.J., 1983. Travel time analysis of borehole seismic data. *J. Geophys. Res.*, 88:8289–8298.
- Stewart, R.R., Huddleston, P.D., and Kan, T.K., 1984. Seismic versus sonic velocities: a vertical seismic profiling study. *Geophysics*, 49:1153–1168.
- Swift, S.A., Hoskins, H., and Stephen, R.A., 1991. Seismic stratigraphy in a transverse ridge, Atlantis II Fracture Zone. In Von Herzen, R.P., Robinson, P.T., et al., *Proc. ODP, Sci. Results*, 118: College Station, TX (Ocean Drilling Program), 219–226.

Date of initial receipt: 17 August 1994

Date of acceptance: 24 February 1995

Ms 148SR-138